Europhysics Letters PREPRINT

## Flow-induced currents in nanotubes: a Brownian dynamics approach

MOUMITA DAS $^{1,2},$  SRIRAM RAMASWAMY $^1,$  A. K.  $\rm SOOD^1$  and G. ANANTHAKRISHNA $^3$ 

- <sup>1</sup> Department of Physics, Indian Institute of Science, Bangalore 560012, India
- <sup>2</sup> Division of Engineering and Applied Sciences, Harvard University, Cambridge, MA-02138.USA.
- <sup>3</sup> Materials Research Centre, IISc, Bangalore 560012, India.

PACS. 02.70.Ns - Molecular dynamics and particle methods.

PACS. 05.10.Gg - Stochastic analysis methods(Fokker-Planck, Langevin, etc).

PACS. 61.46.+w - Nanoscale materials.

Abstract. – Motivated by recent experiments [1] reporting that carbon nanotubes immersed in a flowing fluid displayed an electric current and voltage, we numerically study the behaviour of a collection of Brownian particles in a channel, in the presence of a flow field applied on similar but slower particles in a wide chamber in contact with the channel. For a suitable range of shear rates, we find that the flow field induces a unidirectional drift in the confined particles, and is stronger for narrower channels. The average drift velocity initially rises with increasing shear rate, then shows saturation for a while, thereafter starts decreasing, in qualitative agreement with recent theoretical studies [2] based on Brownian drag and "loss of grip". Interestingly, if the sign of the interspecies interaction is reversed, the direction of the induced drift remains the same, but the flow-rate at which loss of grip occurs is lower, and the level of fluctuations is higher.

Recent experiments show that liquid flow past single walled carbon nanotube (SWNT) bundles generates voltage [1] and electric current [2] in the nanotube, along the direction of flow. The current and voltage are found [1,2] to be highly sublinear functions of the fluid flow rate. The direction of flow-induced current relative to fluid flow is determined [1,2] by the nature of the ions in the vicinity of the nanotubes. The experiments in [1,2] also showed that the one-dimensional nature of the SWNTs was essential for the generation of a net electrical signal in the sample: experiments on graphite did not generate a measurable signal and those on multiwalled carbon nanotubes produced a signal approximately 10 times weaker than that for the single walled nanotubes, the dimensions of the sensing element and flow speeds of the ionic liquid remaining same. Electrokinetic [3] and phonon-wind [4] based explanations give a linear current versus flow rate dependence. There is also a recent proposal [5] involving stick-slip and barrier hopping of ions giving a sublinear dependence. Ghosh et al. [2] explain the phenomenon as follows: Thermal fluctuations in the ionic charge density in the fluid near the nanotube produce a stochastic Coulomb field on the carriers in the nanotube. At thermal equilibrium, i.e., if there is no mean fluid flow, the fluctuation-dissipation theorem tells us

2 EUROPHYSICS LETTERS

that the power spectral density of these fluctuations contributes to the frictional drag on the carriers. The total friction or resistivity of the carriers is thus the sum of contributions from the ambient ions and from phonons or other mechanisms intrinsic to the nanotube. An imposed fluid flow advects the ions. The carriers in the nanotube then have to move at a speed determined by balancing the drag forces due to the ions and the nanotube. However, increasing the fluid velocity also Doppler-shifts the autocorrelation function of the ionic charge density, hence speeding up its time-decay as seen by the carriers and reducing the drag due to the ions. This results in a saturation of the flow-induced voltage and current. The calculation of [2] was done in a simplified framework, where the ions were assumed to move with a single mean velocity. In the experiment the velocity of fluid (and ions) increases with distance from the nanotube surface. Ions nearest the nanotube contribute the strongest Coulomb field but move the slowest. It would be interesting, first, to see if the form of the dependence of current on flow-speed remains intact when these competing tendencies are taken into account. Secondly, it remains to be seen if the theory of [2] produces a weaker effect when extended to flow past a higher dimensional conductor. Lastly, only the two-point correlations of the ionic Coulomb field enter the (Gaussian) treatment of [2], which means that changing the sign of the ionic charge can have no effect. Testing the importance of non-Gaussian fluctuations is important, but hard to do analytically. All three questions are easily resolved in a numerical simulation.

Motivated by these considerations, we carry out a Brownian dynamics study on a model system (Figs. 1) consisting of two types of particles, (i) particles 'A' of low diffusivity in a chamber (ions) and (ii) particles 'B' of comparatively high diffusivity (carriers) confined in an adjoining channel (the nanotube) of depth  $W_B$  much smaller than that of the chamber. Both 'A' and 'B' particles are assumed to be charged particles with pairwise screened Coulomb interactions. Our simulations implement the theoretical ideas of [2] with an important difference: the ions flowing past the nanotube have a strong velocity gradient in the vicinity of the nanotube, as shown in Fig. 1. For a suitable range of shear rates (magnitude of velocity gradient), we find that an imposed flow of the 'A' particles indeed induces a unidirectional drift in the 'B' particles in the channel. The average drift velocity initially rises with increasing shear rate, then shows saturation for a while, and thereafter starts decreasing, in qualitative agreement with the theoretical arguments of [2]. We further observe that the induced drift decreases substantially when  $W_B$  is increased, underlining as in the experiments of [1], the central role of reduced dimensionality. Interestingly, if the sign of the A-B interaction is reversed, the direction of the induced drift remains the same, in agreement with [2], but the flow-rate at which crossover to saturation occurs is lower, and the level of fluctuations is higher.

Model and Results. – Let us now present our study and its results in more detail. We consider for simplicity a two dimensional (x-y) system consisting of two species of particles, say, A representing the ions in the chamber (of dimension  $10\ell \times 10\ell$ , ) and B, representing the carriers in the narrow channel (of dimension  $10\ell \times \epsilon\ell$ ,  $\epsilon \le 2$ ), with  $\ell = (\rho_A)^{-1/2}$ , where  $\rho_A$  is the mean number density of ions. We work with periodic boundary conditions in the x direction, and hard walls at  $y = 10\ell$ , y = 0 and  $y = -\epsilon\ell$ . The flow field imposed on A particles is plane Couette, with velocity in the x direction and gradient in the y direction till a certain separation between the walls  $(5\ell)$ , beyond which the velocity is uniform (Fig. 1). This flow geometry effectively models the flow field near a small obstacle in bulk flow, such that gradients are concentrated in the boundary layer on the surface of the obstacle.

There is no flow field imposed on B particles. Both A and B particles are overdamped and the pairwise interactions are screened Coulomb in nature. Further B particles are 100 times

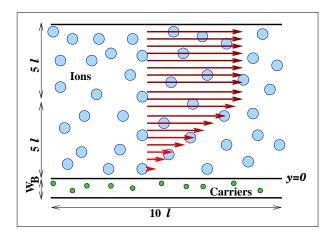


Fig. 1 – A schematic diagram of the model.

more diffusive than their A counterparts. The positions  $\mathbf{R}(t)$  (= x(t), y(t)), evolve according to overdamped Langevin equations, with independent Gaussian, zero-mean, thermal white noise sources  $\mathbf{h_A}$  (or  $\mathbf{h_B}$ ), interparticle forces  $\nabla V$  from the pair potentials, and for the ions an additional force due to the flow field  $\dot{\gamma}\hat{\mathbf{x}}$ . Let us nondimensionalise our variables as follows: scale all lengths by  $\ell$ , energy by Boltzmann's constant  $k_B$  times temperature T (and hence force by  $k_BT/\ell$ ), and time by the time  $\tau$  taken by a carrier to traverse a distance  $\ell$ . Then our nondimensional discretised Langevin equations are for a given type (A or B) of particles,

$$\mathbf{R}_{A}(t+\delta t) = \mathbf{R}_{A}(t) + D_{A}[\dot{\gamma}\hat{\mathbf{x}} - \nabla V_{AA} - \nabla V_{AB}]\delta t + \sqrt{2D_{A}\delta t} \ \mathbf{h}_{\mathbf{A}}(t), \tag{1}$$

$$\mathbf{R}_{B}(t+\delta t) = \mathbf{R}_{B}(t) - D_{B}\nabla V_{BA}\delta t + \sqrt{2D_{A}\delta t} \ \mathbf{h}_{B}(t)$$
 (2)

where  $D_A(=1)$  and  $D_B(=100)$  are the nondimensionalised Brownian diffusivities for the ions and carriers respectively and obey the fluctuation dissipation relation, i.e., for example for A particles,  $\langle \mathbf{h_A}^i(0)\mathbf{h_A}^j(t)\rangle = 2\mathbf{I}\delta^{ij}\delta(t)$ , where I is the unit tensor and i, j label particle indices. The pair potentials have the screened Coulomb form  $V(r) = (U/r) \exp(-\kappa r)$  (where U is a coupling coefficient of the DLVO form (1).) at interparticle separation r, with different  $\kappa$ 's for AA and AB interaction, while there is no BB interaction. Also both the A and B particles carry charges of identical sign and magnitude. The dimensions of the box containing A particles is L=10 and W=10, whereas for B particles L=10, and  $W=\epsilon(\epsilon \leq 2)$ . Keeping  $W_A=10$  and  $\kappa_{AB}\ell=2$  fixed, we monitor the behavior of the system by changing: (1) Width of the channel containing the carriers  $W_B$ , (2) Ion-ion interaction strength,  $\kappa_{AA}\ell$  and (3) sign of the A-B i.e. ion-carrier interaction. We also explore the effect of changing the screening length of the ion-carrier (A - B) interaction, keeping other parameters constant. We have studied the behavior of this model for a system with  $N_A = 100$  particles and  $\rho_A/\rho_B = 1$  and  $\rho_A/\rho_B = 1/2$ ,  $\rho_A$  and  $\rho_B$  being the number densities for the ions and carriers respectively. The results presented here pertain to the latter case, the observed behavior being qualitatively same for both cases.

<sup>(1)</sup> This DLVO coefficient is given by  $Z_i Z_j e^2 exp(\kappa(\sigma_i + \sigma_j))/(\epsilon(1 + \kappa \sigma_i)(1 + \kappa \sigma_j))$ , where  $\epsilon$  is the dielectric constant of the solvent,  $Z_i e$  is the charge on and  $\sigma_i$  is the radius of the  $i^{th}$  particle. In our simulations, the dimensionless value of the  $\kappa$  independent part of U is  $\approx 15.3$ ,  $\sigma_B/\sigma_A = 0.1$  and  $2\sigma_A/\ell \approx 0.455$ .

4 EUROPHYSICS LETTERS

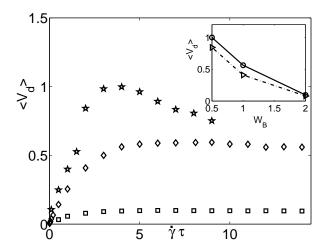


Fig. 2 – The induced drift of the carriers as a function of the ionic flow speed for different  $W_B$  (stars, diamonds and squares correspond to  $W_B = 0.5, W_B = 1.0$  and  $W_B = 2.0$  respectively) for  $\kappa_{AA}\ell = 1$ . The inset shows the average drift velocity  $\langle v_d \rangle$  as a function of  $W_B$ , for  $\dot{\gamma}\tau = 4.0$  (circles) and 2.0 (triangles) respectively.

For  $W_B = 2$ , we observe that the carriers do have a unidirectional drift in the direction of the flow. The average drift velocity of the carriers initially increases with the flow rate, reaches a maximum and then decreases at large values of the flow rate as seen in Fig. 2. This is broadly in agreement with the ideas of [2]. On further decreasing  $W_B$  to first 1.0 and then 0.5 (Fig.2), we find that the drift velocity induced is progressively larger than for  $W_B = 2.0$ , and the saturation occurs at a lower value of the flow rate.

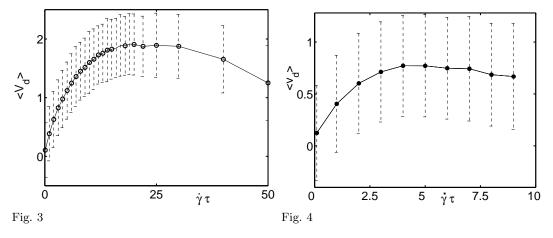


Fig. 3 – Induced drift as function of flow speed for  $\kappa_{AA}\ell=0.2$ ,  $W_B=0.5$ . The vertical dashed lines show the standard deviation from the mean drift velocity.

Fig. 4 – Induced drift as function of flow speed for  $\kappa_{AA}\ell=4$ ,  $W_B=0.5$ . Note that the velocity weakening takes place at a much smaller shear rate than in Fig.3. The vertical dashed lines show the standard deviation from the mean drift velocity.

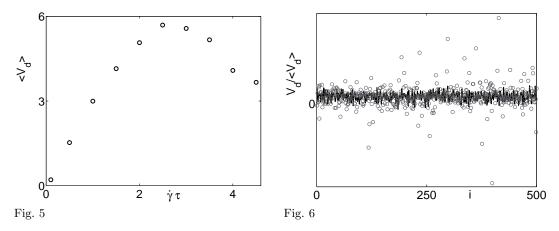


Fig. 5 – Induced drift as a function of the ionic flow speed for  $\kappa_{AA}\ell=1$ ,  $W_B=1$ , with attractive ion-carrier interaction.

Fig. 6 – Drift velocities  $V_d$  of the carriers at different times (represented by the index 'i') scaled by the average value  $\langle V_d \rangle$  at  $\kappa_{AA}\ell = 1$ ,  $W_B = 1$ , for repulsive (lines) and attractive (circles) ion-carrier interactions.

Now keeping the wall to wall distance fixed at  $W_B = 0.5$ , we study the behavior of the system at very small  $(\kappa_{AA}\ell=0.2)$  (Fig. 3)and large  $(\kappa_{AA}\ell=4)$  ion-ion interaction screening strength (Fig. 4). A smaller value of  $\kappa\ell$  corresponds to stronger ion-ion interactions and it is observed that in such a case the induced effect on the carriers is stronger and is sustained till a larger value of the ionic flow speed at which the weakening sets in.

We now look at the scenario where the two species A (ions) and B (carriers) have opposite charges (Fig. 5). The wall to wall distance is kept fixed at  $W_B = 1$ . We observe that the induced drift is stronger than when both A and B particles carry like charges, at the same  $W_B$ . The fluctuations in the drift velocity are however much larger than for the case of like charges (Fig. 6): the ratio of standard deviation to mean is  $\sim 4$  times that for the repulsive case. This can be explained as follows: The attraction of the carriers for the ions brings both close to the wall separating them, from time to time, enhancing the flow induced current. Subsequently the presence of the walls pushes them apart, reducing the induced current again. This implies large fluctuations in the current. For like charged ions and carriers both the Coulomb repulsion and the walls act in tandem to keep them apart, thus the intermittent enhancement and reduction in current does not occur.

In order to understand the dependence of the effect on the strength of A-B interaction, we monitored the system for different values of the screening length corresonding to the A-B interaction (Fig. 7) keeping the channel width  $W_B$  and A-A interaction strength constant. We find that the effect increases on increasing the screening length  $\kappa_{AB}^{-1}$  and is maximum where  $\kappa_{AB}^{-1}$  is comparable to the width of the channel  $W_B$ ; therafter it saturates and doesn't show a marked increase. This shows that the contribution to the flow induced effect indeed chiefly comes from the A particles (or ions) present in a boundary layer of order of the width of the channel at the interface of the chamber and the channel.

We observe that our simulations (Fig. 8) agree well with the theoretical predictions of a saturating dependence of the induced velocity of the carriers on the imposed flow speeds (Fig. 9). We further find the current decreases when  $\dot{\gamma}$  passes a threshold value  $\dot{\gamma}_c$ , and that  $\dot{\gamma}_c$  is

6 EUROPHYSICS LETTERS

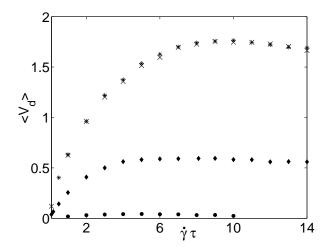


Fig. 7 – The flow induced drift velocity of B particles as a function of the flow speed of A particles, for  $\kappa_{AB}^{-1} = 0.1\ell$  (circles),  $0.5\ell$  (diamonds),  $5\ell$  (cross) and  $10\ell$  (plus), for fixed  $W_B = 1.0$  and  $\kappa_{AA}\ell = 1$ .

smaller for smaller  $W_B$ . This observation demands a theoretical explanation which at present we do not have. We hope this will motivate further experiments to check this prediction. It is significant that we are able to observe this type of "Brownian drag" and transfer of momentum even in the absence of momentum conservation and in the extreme limit of no inertia. Also, though strictly speaking fluctuation dissipation relations are valid only in equilibrium, a naive extension of FDT as in [2] to the flowing case would imply a decrease in the rate of relaxation with increasing flow rate, and hence a "loss of grip" and a velocity weakening, which is what we find.

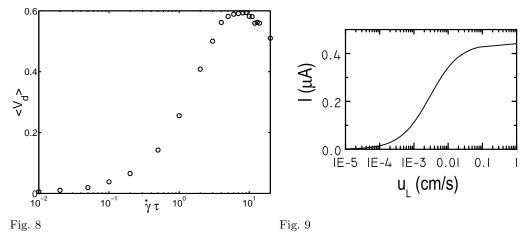


Fig. 8 – Induced velocity with flow speed for parameter values as in Fig. 3 on a log scale for comparison with the behavior predicted by [2] as shown in Fig. 9.

Fig. 9 – Current I as a function of flow speed  $u_L$ . Figure provided by [2].

\* \* \*

We thank S. Ghosh for useful discussions and providing figure 9. MD acknowledges CSIR, India for support, and SR and GA thank the DST, India for support through the Centre for Condensed Matter Theory. AKS thanks DST for financial support of his research on carbon nanotubes.

## REFERENCES

- [1] S. GHOSH, A.K. SOOD AND N. KUMAR, Science, 299 (2003) 1042.
- [2] S. Ghosh, A.K. Sood, Sriram Ramaswamy and N. Kumar, *Phys. Rev. B*, **70** (2004) 205423
- [3] A. E. COHEN (COMMENT); S. GHOSH, A. K. SOOD, AND N. KUMAR (REPLY), Science, **300** (2003) 1235.
- [4] P. Kral and M.Shapiro, Phys. Rev. Lett., 86 (2001) 131
- [5] B. N. J. Persson, U. Tartaglino, E. Tosatti, and H. Ueba, Phys. Rev. B, 69 (2004) 235410